

## *Retraction*

# **Retracted: Preparation of Mg<sub>2</sub>Ni Hydrogen Storage Alloy Materials by High Energy Ball Milling**

### **Advances in Materials Science and Engineering**

Received 26 December 2023; Accepted 26 December 2023; Published 29 December 2023

Copyright © 2023 Advances in Materials Science and Engineering. This is an open access article distributed under the Creative Commons Attribution License, which permits unrestricted use, distribution, and reproduction in any medium, provided the original work is properly cited.

This article has been retracted by Hindawi, as publisher, following an investigation undertaken by the publisher [1]. This investigation has uncovered evidence of systematic manipulation of the publication and peer-review process. We cannot, therefore, vouch for the reliability or integrity of this article.

Please note that this notice is intended solely to alert readers that the peer-review process of this article has been compromised.

Wiley and Hindawi regret that the usual quality checks did not identify these issues before publication and have since put additional measures in place to safeguard research integrity.

We wish to credit our Research Integrity and Research Publishing teams and anonymous and named external researchers and research integrity experts for contributing to this investigation.

The corresponding author, as the representative of all authors, has been given the opportunity to register their agreement or disagreement to this retraction. We have kept a record of any response received.

### **References**

- [1] X. Liu, L. Zhou, W. Li et al., "Preparation of Mg<sub>2</sub>Ni Hydrogen Storage Alloy Materials by High Energy Ball Milling," *Advances in Materials Science and Engineering*, vol. 2022, Article ID 2661424, 8 pages, 2022.

## Research Article

# Preparation of Mg<sub>2</sub>Ni Hydrogen Storage Alloy Materials by High Energy Ball Milling

Xusheng Liu , Lei Zhou , Wenhao Li, Shaopeng Wu, Qinglan Huang, Yankun Wang, and Xiaolan Cai

Faculty of Metallurgical and Energy Engineering, Kunming University of Science and Technology, Kunming 650093, China

Correspondence should be addressed to Lei Zhou; [zhoulei@kust.edu.cn](mailto:zhoulei@kust.edu.cn)

Received 5 May 2022; Accepted 26 May 2022; Published 11 July 2022

Academic Editor: Haichang Zhang

Copyright © 2022 Xusheng Liu et al. This is an open access article distributed under the Creative Commons Attribution License, which permits unrestricted use, distribution, and reproduction in any medium, provided the original work is properly cited.

In this paper, Mg<sub>2</sub>Ni hydrogen storage alloy powder was prepared by high-energy ball milling mechanical alloying method, and the influence of stirring shaft rotation speed, ball milling time, and different sizes of ball mills on the formation time, powder morphology, and crystal structure of Mg<sub>2</sub>Ni alloy during ball milling was studied. The results show that the Mg<sub>2</sub>Ni alloy was obtained by high-energy ball milling in this work, and the efficiency was increased by about 76% compared with the traditional ball milling method. In the case of higher rotational speed or larger blades, the time to generate Mg<sub>2</sub>Ni alloy can be advanced, the alloying process can be shortened, and Mg<sub>2</sub>Ni alloy with a particle size of less than 10 μm can be obtained. However, after the ball milling reaches a certain time, the cold welding and crushing of the alloy powder reach a balance, and the particle size is basically unchanged. The hydrogen storage alloy was activated, the hydrogen storage PCT curve was detected, and the hydrogen absorption kinetic curve and the PCT curve were analyzed. After ball milling at 900/1100 rpm for 13 hours, a Mg<sub>2</sub>Ni alloy with a single composition, extremely low impurity content, and partially amorphous and nanocrystalline coexistence was obtained. Its mass hydrogen storage density also reached the theoretical value of 3.6 wt%.

## 1. Introduction

Although magnesium-based hydrogen storage alloys have defects such as high hydrogen absorption and desorption temperature and slow hydrogen absorption and desorption rates, they are considered to be the most promising light-weight hydrogen storage alloys due to their high hydrogen storage capacity, abundant resources, and low cost. In magnesium-based hydrogen storage alloys, magnesium-based hydrogen storage alloys containing single-phase or multiphase can be prepared by compounding Mg with metal elements dominated by transition metals. The existence of the alloy can promote the adsorption and dissociation of hydrogen, while the multiphase boundary can provide a large number of nucleation sites for sample hydrogenation and dehydrogenation, reduce the stability of MgH<sub>2</sub>, and improve the hydrogen storage performance of the sample [1–3]. The addition of nickel to magnesium is beneficial in many aspects. The most important point is the ability to

form alloys with magnesium. In general, MgNi alloys exhibit enhanced adsorption kinetics [4]. The combination of Mg and Ni can form a Mg<sub>2</sub>Ni intermetallic compound with excellent hydrogen absorption and desorption properties [5–10]. Mg<sub>2</sub>Ni preferentially absorbs a small amount of hydrogen during the hydrogen absorption process to form a Mg<sub>2</sub>NiH<sub>0.3</sub> solid solution and continues to absorb hydrogen to obtain Mg<sub>2</sub>NiH<sub>4</sub>. This reaction is reversible under the right conditions.

Magnesium-based hydrogen storage alloys represented by Mg<sub>2</sub>Ni have the advantages of large hydrogen storage capacity, abundant resources, and low price [11]. Since Mg<sub>2</sub>Ni alloy was synthesized in 1964, it has higher hydrogen storage capacity (3.6 wt%), milder reversible hydrogen absorption/desorption temperature, and better hydrogen storage kinetics than pure Mg and other magnesium alloys. It is considered to be the most promising hydrogen storage alloy [12]. The PCT data of Mg<sub>2</sub>Ni show that it has a large hydrogen absorption capacity and a platform slope of 0.02.

Hydrogen is absorbed in 523 K and can be released at 573 K. The formation enthalpy of  $\text{Mg}_2\text{Ni}$  hydrogen absorption to form  $\text{Mg}_2\text{NiH}_4$  is  $-64.5$  kJ/mol, and the entropy is  $-122$  kJ/mol  $\text{H}_2$  [13]. When H atoms enter the interstitial position of the  $\text{Mg}_2\text{Ni}$  lattice, the  $\alpha$  phase will be formed, and the crystal structure will not change at this time; after the complete transformation into the  $\alpha$  phase, continuous hydrogen absorption will cause a phase transition reaction to generate  $\beta$  phase. In the temperature range of 518~483 K,  $\text{Mg}_2\text{NiH}_4$  will transform from the high-temperature phase of the cubic structure to the low-temperature phase of the monoclinic structure [14]. Until now, a large number of researches on magnesium-based hydrogen storage materials are still focused on hydrogen storage materials based on  $\text{Mg}_2\text{Ni}$  alloys.

To improve the hydrogen absorption rate of  $\text{Mg}_2\text{Ni}$ , preactivation treatment is required. This activation treatment is usually very complicated. For elements whose melting points are too different in hydrogen storage alloys, it is difficult to obtain the most accurate alloy by melting method. The mechanical alloying method (MA) [15, 16] avoids melting the metal, which is also an efficient method for refining magnesium-based hydrogen storage materials, actually a high-energy ball milling process. Refinement of magnesium-based hydrogen storage materials can significantly improve their hydrogen absorption and desorption kinetics. The fine particle size can shorten the diffusion distance of hydrogen atoms, and a large number of grain boundaries and phase boundaries can be used as nucleation sites for new phases in the process of hydrogen absorption and desorption. And the diffusion channel of hydrogen atoms accelerates the process of hydrogen absorption and desorption. The mechanical alloying method can be carried out at room temperature without heating and can be directly prepared from the solid-state without melting at a lower temperature. In this process, different powders are rolled and welded by grinding balls with large kinetic energy to form multilayer composite particles with a certain atomic bonding force between the layers. The mechanical energy can diffuse the atoms of one element into another matrix to achieve the purpose of alloying. With the continuous refinement and entanglement of the layered structure in the composite particles, the degree of alloying will become higher and higher, which will promote the formation of amorphous and metastable phases, thereby changing the structure and proportion of the alloy powder and the obtained alloy uniformity. Alloy refinement after high-energy ball milling will increase the contact area between the material and hydrogen; at the same time, lattice defects will also increase, which greatly improves the hydrogen absorption and desorption performance of magnesium-based hydrogen storage materials. Ono et al. used the mechanical alloying method to study the effect of Ni content in Mg-Ni composites on their hydrogen absorption kinetics. It is found that the addition of Ni can significantly increase the hydrogen absorption reaction rate of the composites and at the same time improve the reversible hydrogen storage properties of the composites. This lays the foundation for the subsequent mechanical alloying of magnesium-based hydrogen storage alloys. It takes more than 55 h to grind a

relatively complete  $\text{Mg}_2\text{Ni}$  alloy by traditional high-energy ball milling [17]. The horizontal high-energy ball mill used in this paper has greatly improved the ball milling efficiency, and the time for the complete synthesis of  $\text{Mg}_2\text{Ni}$  alloy has been increased to 15 h at the fastest.

## 2. Experimental

*2.1. Experimental Process.* In this experiment, a horizontal stirring 1 L high-energy ball mill (1 L capacity, HCX-1) and a 2 L high-energy ball mill (2 L capacity, HCX-2) produced by Kunming Haichuangxing Company were used for comparative experiments. The ball milling process parameters used in this experiment are shown in Tables 1 and 2. The main difference between the two ball mills is that the blade size of HCX-2 is double the size of the HCX-1 blade. In the glove box, weigh 60 g of magnesium powder (purity 99.5%, particle size 200 mesh) and nickel powder 50 g (purity 99.5%, particle size 200 mesh) calculated according to the molar ratio and the ball-to-material ratio. Mix evenly and put it into a high-energy ball mill, turn on the circulating cooling water, control the temperature in the chamber at  $30^\circ\text{C}$ , and carry out the whole process of ball milling under the protective atmosphere of argon. The diameter of the stainless-steel balls used in the ball milling is 3 mm, the rotation speed is alternated for 1 minute during the ball milling, and the machine is stopped for 10 minutes for cooling every 60 minutes. By continuously changing the moving speed of the rotor and the grinding ball, it can not only prevent the temperature from being too high but also break the movement balance between the grinding ball and the powder and change the moving position of the grinding ball and the powder in the cabin. Avoid always colliding and hitting the same part, resulting in the accumulation of powder to achieve the purpose of reducing welding. The selection is carried out under different rotational speeds and different blades of different ball mills, and the control agent used in the process is stearic acid.

*2.2. Characterization.* The  $\text{Mg}_2\text{Ni}$  hydrogen storage alloy was characterized by X-ray diffractometer (XRD, Rigaku, D/MAX-2500H) to determine the time process of the formation of the  $\text{Mg}_2\text{Ni}$  alloy. Scanning electron microscope SEM (Zeiss, Gemini300) was used to observe the micro-morphology and particle size of the powder. Transmission electron microscope TEM (FEI Tecnai G2F20) was used to determine that the substance in XRD was  $\text{Mg}_2\text{Ni}$  and observe the changes in crystal phase and lattice. Siverts automatic PCT hydrogen storage detector obtains the hydrogen absorption and desorption kinetics and PCT curve of  $\text{Mg}_2\text{Ni}$  alloy and analyzes the hydrogen storage performance of the sample.

## 3. Results and Discussion

*3.1. Phase Composition.* Combined with the PDF card data, the XRD patterns of the experimental samples of the 1 L ball mill at a high rotation speed in four time periods were analyzed. It can be seen from Figure 1 that the diffraction

TABLE 1: Milling process parameters of HCX-1.

Milling time (h)	Speed (rpm)	Ball-to-powder ratio	Process control agent
9	1600/1800	15:1	Stearic acid
13	1600/1800	15:1	Stearic acid
17	1600/1800	15:1	Stearic acid
21	1600/1800	15:1	Stearic acid
13	900/1100	15:1	Stearic acid

TABLE 2: Milling process parameters of HCX-2.

Milling time (h)	Speed (rpm)	Ball-to-powder ratio	Process control agent
7	900/1100	15:1	Stearic acid
9	900/1100	15:1	Stearic acid
11	900/1100	15:1	Stearic acid
13	900/1100	15:1	Stearic acid

peaks of the samples after ball milling for 9 hours are sharp, the main phase is fcc phase metal Ni, followed by the original hexagonal metal Mg, and the characteristic peaks of  $Mg_2Ni$  begin to appear. The XRD diffraction pattern of the sample after ball milling for 13 h is similar to that of the sample after ball milling for 9 h. The main phase is still Ni, followed by metal Mg and alloy  $Mg_2Ni$ , and the peak intensities of Ni and Mg in the main phase are weakened. The characteristic peaks of  $Mg_2Ni$  are enhanced. Continue to perform ball milling for 17 h, and the XRD pattern has a great change compared with the spectra of 9 h and 13 h. Other characteristic peaks of  $Mg_2Ni$  begin to form in the near-angle range of the Ni peak, and the main term becomes  $Mg_2Ni$ . Secondly, there is the existence of the Ni phase, but the intensity of characteristic peaks has been significantly reduced, and the metallic Mg phase has almost disappeared. After 21 h of ball milling, the characteristic peaks of Mg and Ni disappeared, and only two weak characteristic peaks remained, and the main phase was  $Mg_2Ni$ , which indicated that the  $Mg_2Ni$  alloy was formed completely after 21 h of ball milling.

Figure 2 shows the XRD pattern of HCX-1 ball-milled at 900/1100 rpm for 13 h. Analysis of Figure 2 shows that the XRD pattern has only the Mg phase and Ni phase without the production of  $Mg_2Ni$  alloy. Compared with the XRD of the ball mill at 1600/1800 rpm for 9 h, the efficiency is lower. Therefore, the formation time of  $Mg_2Ni$  alloy has a great relationship with the rotation speed. When the rotation speed of the 1L ball mill was 1600/1800 rpm, a large amount of  $Mg_2Ni$  began to be produced at 13 h, and there was still a small amount of nickel residue after ball milling for 21 h. However, the 1L ball mill still does not produce  $Mg_2Ni$  alloy after 13 h of ball milling at 900/1100 rpm. Therefore, at a higher rotational speed, the larger collision energy between the steel ball and the powder can advance the time for the formation of  $Mg_2Ni$  alloy. It is beneficial to improve the ball milling efficiency.

It can be seen from Figure 3 that the peak shapes of the XRD patterns of HCX-2 after ball milling for 7 h and HCX-1 for 13 h are similar. After HCX-2 was milled for 7 h, a large amount of  $Mg_2Ni$  alloy began to be produced, and the Mg phase had basically disappeared, and the main phase was Ni, followed by  $Mg_2Ni$  alloy. After HCX-2 was milled for 9 h, the

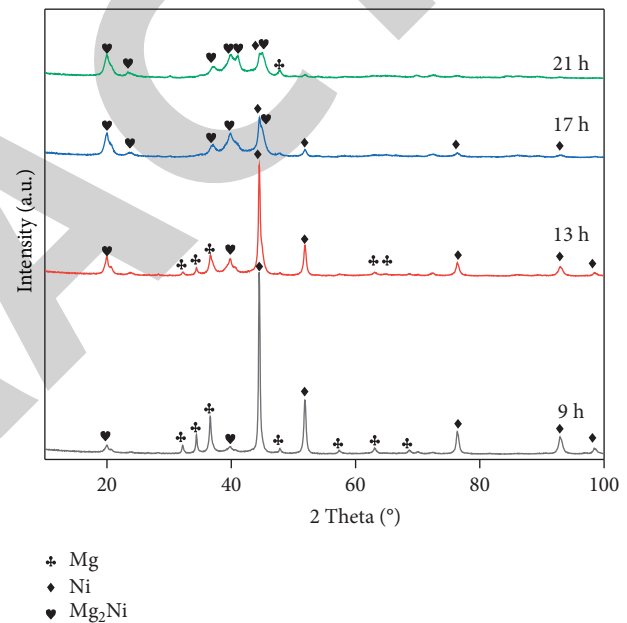


FIGURE 1: XRD patterns of HCX-1 ball mill at 1600–1800 rpm for 21 h, 17 h, 13 h, and 9 h.

intensity of the characteristic peaks of Ni decreased significantly, and the main phase changed to  $Mg_2Ni$  alloy, which was similar to the peak shape of HCX-1 milled for 21 h. After ball milling for 11 h, the elemental peaks of Mg and Ni basically disappeared, and the impurity content of  $Mg_2Ni$  alloy was less. After continuing ball milling for 13 h, the strength of the Ni peak has basically disappeared, and only a large amount of  $Mg_2Ni$  alloy remains.

The initial stage of ball milling is mainly due to the collision and friction between the grinding medium and the raw powder, the powder is deformed, the grains are refined, and the diffraction peaks are broadened. The main phases are metal nickel with fcc structure and metal magnesium with original hexagonal structure. With the progress of ball milling, mechanical alloying occurs to form  $Mg_2Ni$  alloy, but due to different process conditions in each experiment, the time for mechanical alloying to occur is different and the



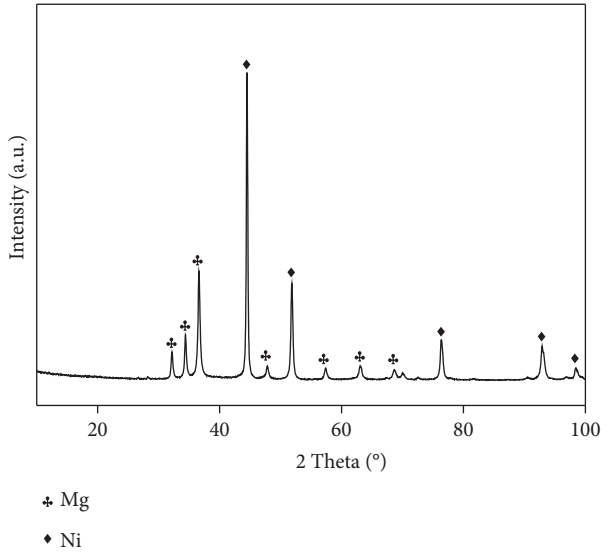


FIGURE 2: XRD pattern of HCX-1 ball milling at 900–1100 rpm for 13 h.

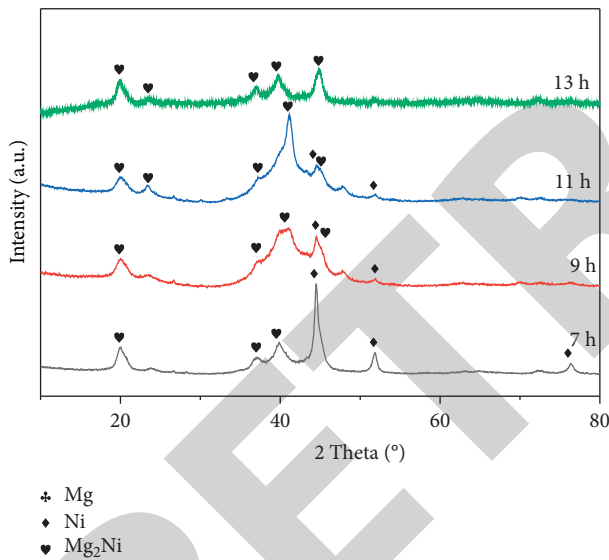


FIGURE 3: XRD patterns of HCX-2 ball milling for 7 h, 9 h, 11 h, and 13 h.

final degree of complete alloying is also different. According to the research on high-energy ball mills by the German ZOZ company [18], the energy ( $E_{\text{powder}}$ ) obtained by powder during ball milling can be expressed by the following formula:

$$E_{\text{powder}} \text{const} \equiv P_1 t_1 = P_2 t_2 \equiv \frac{P_1}{P_2} = \frac{t_2}{t_1}. \quad (1)$$

The energy ( $E_{\text{powder}}$ ) delivered to the powder is a function of power ( $P$ ) and time ( $t$ ), which is directly related to the speed of the rotor. From the above formula, it can be seen that the results obtained by ball milling for a short time at a higher speed are the same as those for a long time at a low speed. The speed reduction reduces the energy

transferred from the rotor to the grinding media and ultimately to the powder in the same amount of time, increasing the time required for alloying. Likewise, the size of the blades during ball milling also affects the power transfer from the rotor to the grinding media. As the blades increase, the energy transferred from the rotor to the grinding media and ultimately to the powder at the same time increases, and the time required for alloying decreases.

When the rotating speed of HXC-2 was 900/1100 rpm, a large amount of  $\text{Mg}_2\text{Ni}$  began to be produced after 7 h of ball milling. After 13 h of ball milling, there was not much nickel left, and the main phase was  $\text{Mg}_2\text{Ni}$ . According to formula (1), it can be known that the time for the formation of  $\text{Mg}_2\text{Ni}$  alloy in the ball milling process is not only related to the rotational speed but also the size of the blade of the ball mill. The leaves of HXC-2 are twice as large as those of HXC-1. The efficiency of HXC-2 is significantly higher when the speed is the same. When the speed of HXC-1 reaches 1600/1800 rpm, the efficiency is still not as high as that of HXC-2 at 900/1100 rpm, so it can be seen that the size of the blade has a greater impact on the ball milling process. When the blade is larger, the time to form the alloy is advanced and the alloying process is shortened. Through this experiment, it can be seen that the time for ball milling of  $\text{Mg}_2\text{Ni}$  hydrogen storage alloy by horizontal high-energy ball mill is 13 h, which greatly improves the ball milling efficiency compared with the traditional ball milling of hydrogen storage alloy.

**3.2. Microstructure Analysis.** It can be seen from the SEM morphology of the samples at each stage of HXC-1 ball milling shown in Figure 4 that the powder particle size distribution in the primary stage of ball milling is relatively broad. This is because the ductile component magnesium forms a lamellar structure under the action of ball milling, while the brittle nickel is pulverized and the powder is refined resulting in an uneven particle size distribution. It can be seen from Figure 4(b) that the particle size does not change greatly with the ball milling, and these particles have a layered composite structure. This is because the brittle nickel particles are broken and embedded in the matrix formed by the ductile component magnesium under the impact and friction of the grinding medium. Large particles are larger than 10  $\mu\text{m}$  in size. After 17 h of ball milling, it can be seen from the figure that the longer the time is, the greater the hardening stress of the metal is. At this time, the crushing of the metal powder is greater than that of the cold welding, so the particle size becomes smaller. After 21 h of ball milling, the particle size of the obtained powder was relatively uniform, the particle size remained at about 10  $\mu\text{m}$ , and the particle shape was polygonal or irregular.

Figure 5 is similar to Figure 4. The particle size of HXC-2 in the early stage of ball milling is large and the distribution is not uniform. Until about 13 h of ball milling, the particle size of the powder is relatively uniform, the particle size is also maintained at about 10  $\mu\text{m}$ , and the particles are polygonal or irregular. During the ball milling process, the particle size no longer decreases with the increase of ball milling time. The particle size is always kept around 10  $\mu\text{m}$ .

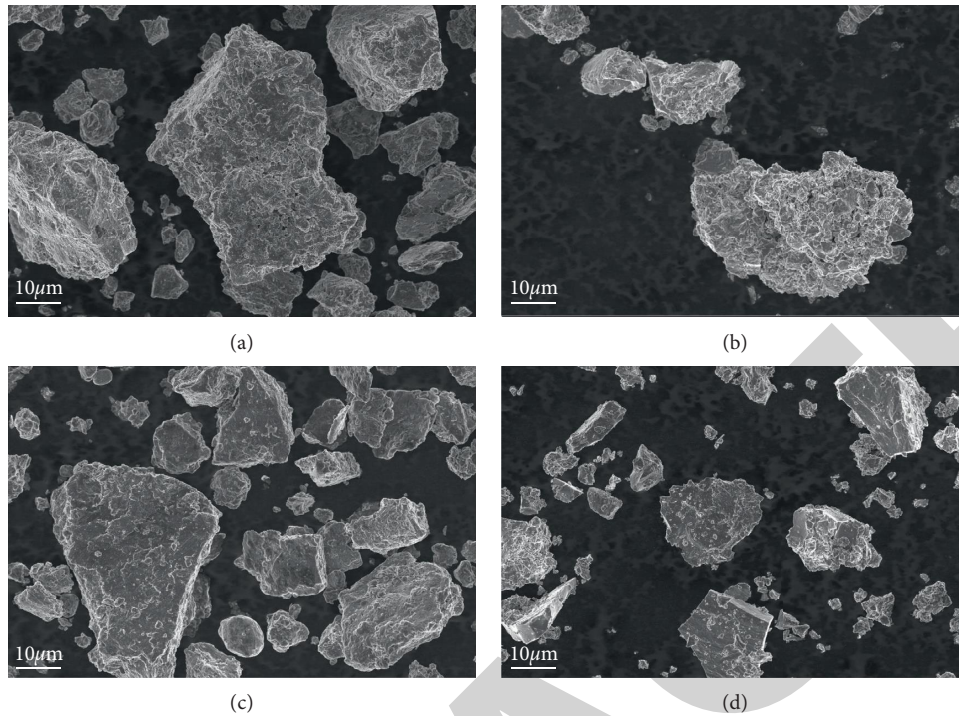


FIGURE 4: SEM image of HCX-1 ball milling: (a) 9 h; (b) 13 h; (c) 17 h; (d) 21 h.

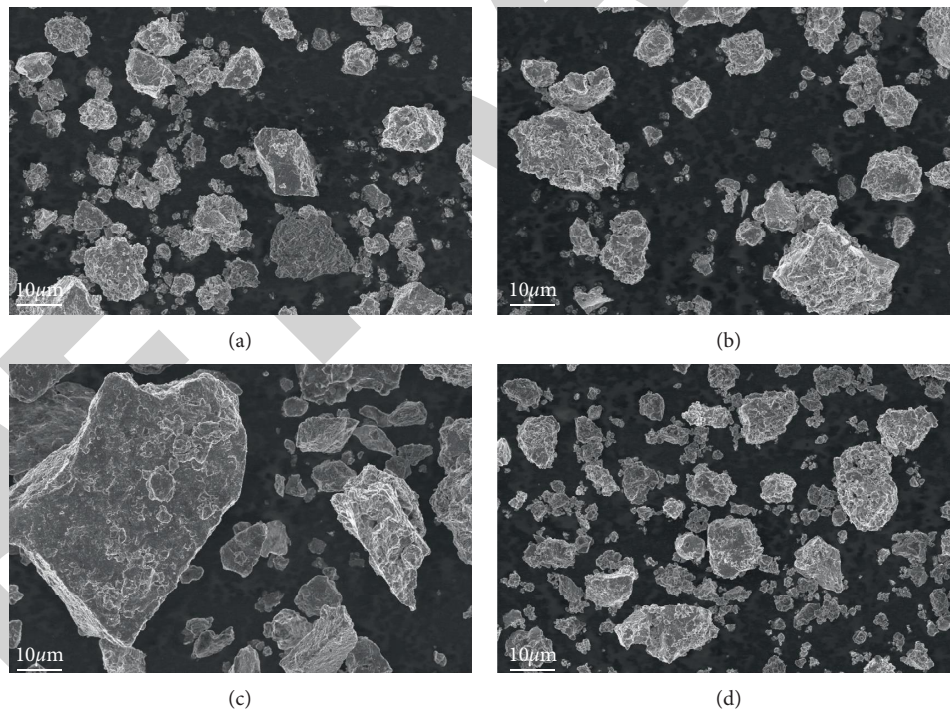


FIGURE 5: SEM image of HCX-2 ball milling: (a) 7 h; (b) 9 h; (c) 11 h; (d) 13 h.

This is because the powder has been ball milled for a long time to achieve a balance between particle crushing and cold welding.

Figure 6 is the high-resolution TEM morphology of HCX-1 after ball milling for 21 h. It can be seen from the two sets of high-magnification transmission electron microscopes that overall the alloys coexist with amorphous and

crystalline, and there is agglomeration. The crystal plane of  $Mg_2Ni$  is obtained by the analysis of the interplanar spacing, and it can be seen that most of the crystal planes are  $Mg_2Ni$  (203) crystal planes.

Figure 7 is the high-resolution TEM morphology of HCX-2 after ball milling for 13 h. Generally speaking, the  $Mg_2Ni$  alloys obtained by ball milling of HCX-2 are mostly



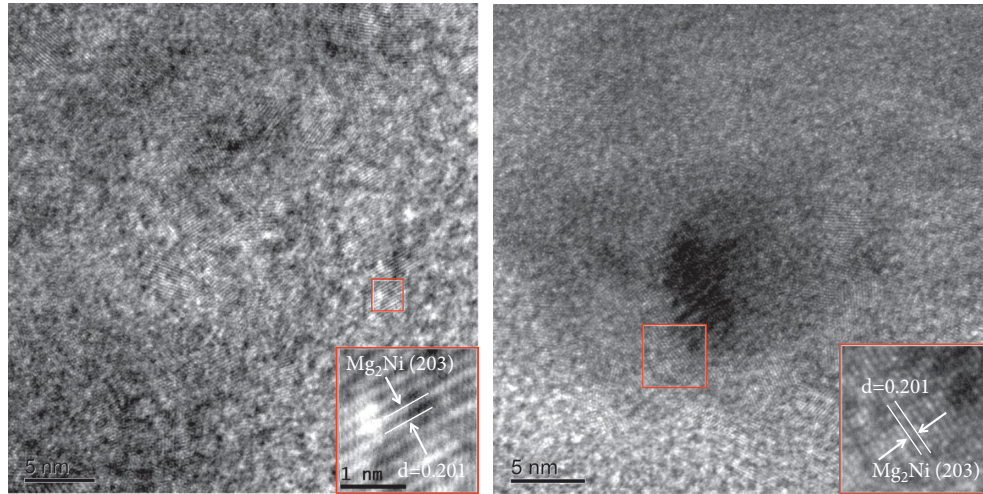


FIGURE 6: TEM image of HXC-1 ball milling for 21 h.

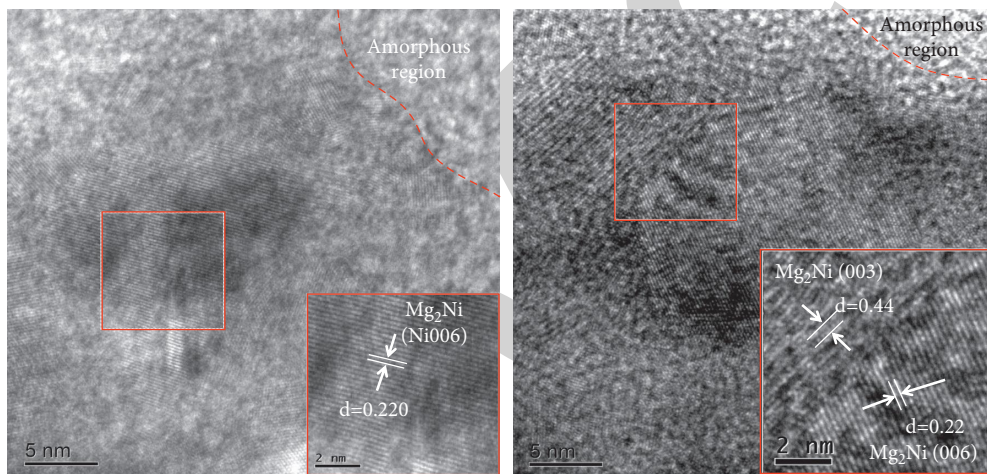


FIGURE 7: TEM image of HXC-2 ball milling for 13 h.

alloys of the  $\text{Mg}_2\text{Ni}(006)$  crystal plane, which is different from those of HXC-1. This may be because the HXC-2 blade is larger and the collision energy is higher, so  $\text{Mg}_2\text{Ni}$  alloys with different crystal planes are obtained, and there is also a small amount of amorphous agglomeration.

**3.3. Hydrogen Storage Performance.** The hydrogen storage properties of the alloys were tested on a semiautomatic PCT tester. Before the test, the sample should be put at  $300^\circ\text{C}$ , under the hydrogen pressure of 3 MPa to make the material saturated with hydrogen once. Then, the material was activated by degassing hydrogen once in a vacuum state of  $300^\circ\text{C}$ . Activation is to enable the sample to achieve its proper hydrogen absorption and desorption rate and hydrogen storage capacity. After the activation is completed, the sample can be tested for PCT hydrogen absorption and desorption performance.

Figure 8 is the kinetic curve of the first activation of hydrogen absorption of the finished  $\text{Mg}_2\text{Ni}$  alloy after ball milling by the ball mill. The hydrogen storage capacity reached 3.1 wt% during the first activation of hydrogen absorption. Subsequently, the PCT test was carried out, and the PCT curve of hydrogen absorption and desorption at  $300^\circ\text{C}$  was obtained as shown in Figure 9. The PCT curve of the alloy has a flat and broad plateau region, which is favorable for hydrogen storage, and the hydrogen storage capacity reaches the theoretical value of 3.6 wt%. Combined with XRD and high-resolution transmission analysis, it is known that the  $\text{Mg}_2\text{Ni}$  prepared by high-energy ball milling has a single composition and low impurity content and contains a small amount of crystal structure with the coexistence of amorphous and nanocrystalline. Therefore,  $\text{Mg}_2\text{Ni}$  hydrogen storage alloys with higher purity and better crystal structure can be obtained with higher efficiency through our high-energy ball milling method.

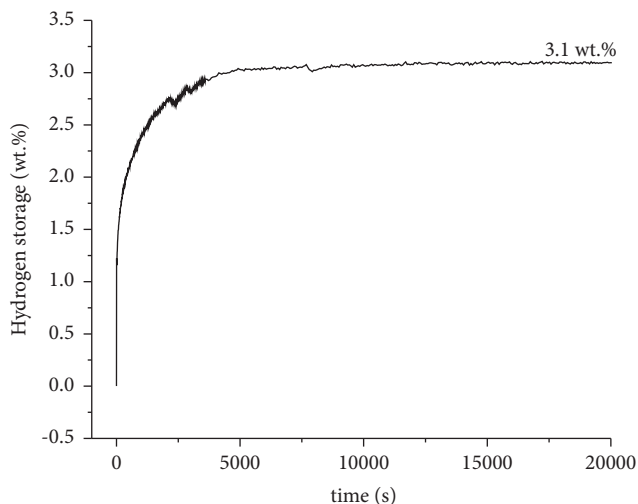


FIGURE 8: The kinetic curve of first activated hydrogen absorption after ball milling.

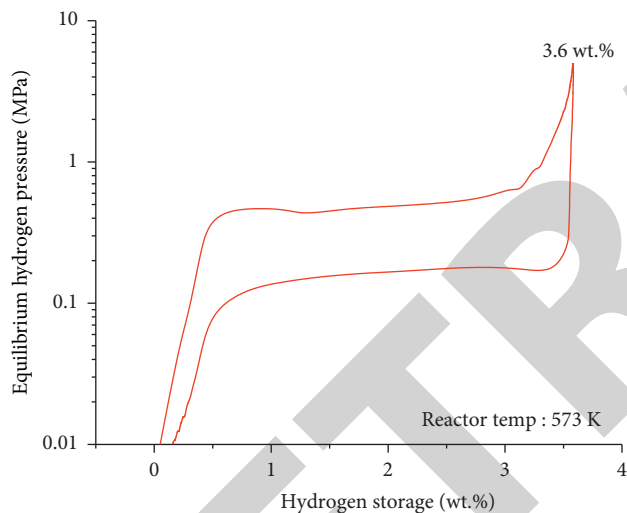


FIGURE 9: PCT curve of  $Mg_2Ni$  hydrogen storage alloy obtained by ball milling.

#### 4. Conclusion

In this paper,  $Mg_2Ni$  hydrogen storage alloy materials were prepared by high-energy ball milling. Through analysis, it is obtained that ball milling can advance the formation time of  $Mg_2Ni$  alloy and shorten the process of complete alloying under the condition of ball milling at higher rotational speed or increasing the number of ball-milled blades. The traditional ball milling of  $Mg_2Ni$  alloy requires more than 55 h of ball milling time, and the horizontal high-energy ball mill used in this experiment greatly improves the synthesis efficiency of  $Mg_2Ni$  alloy. Its efficiency is increased by about 76%. During the continuous ball milling of the high-energy ball mill, the particle size did not change much and finally stayed at about 10  $\mu m$ . This is because the crushing and welding of the powder have reached a balance after a long period of ball milling with high collision energy. The crystal grains are polygonal or irregular in shape, and there is also a small amount of amorphous and agglomerated phenomena.

#### Data Availability

The data used to support the findings of this study are included within the article.

#### Conflicts of Interest

The authors declare that they have no conflicts of interest.

#### Acknowledgments

This work was financially supported by the Program for Innovative Research Team (in Science and Technology) in the University of Yunnan Province (No. 14051693) and the Basic Research Project of Yunnan Province (No. 202001AS070049 and No. 202102AB080004).

#### References

- [1] J. Zhang, Y. Zhu, X. Zang et al., "Nickel-decorated graphene nanoplates for enhanced  $H_2$  sorption properties of magnesium hydride at moderate temperatures," *Journal of Materials Chemistry*, vol. 4, no. 7, pp. 2560–2570, 2016.
- [2] M. G. Verón, H. Troiani, and F. C. Gennari, "Synergetic effect of Co and carbon nanotubes on  $MgH_2$  sorption properties," *Carbon*, vol. 49, no. 7, pp. 2413–2423, 2011.
- [3] X. Huang, X. Xiao, W. Zhang et al., "Transition metal (Co, Ni) nanoparticles wrapped with carbon and their superior catalytic activities for the reversible hydrogen storage of magnesium hydride," *Physical Chemistry Chemical Physics*, vol. 19, no. 5, pp. 4019–4029, 2017.
- [4] J. Matsuda, K. Yoshida, Y. Sasaki, N. Uchiyama, and E. Akiba, "In situ observation on hydrogenation of Mg-Ni films using environmental transmission electron microscope with aberration correction," *Applied Physics Letters*, vol. 105, no. 8, p. 083903, 2014.
- [5] X. Hou, R. Hu, Y. Yang, L. Feng, and G. Suo, "Modification based on internal refinement and external decoration: a powerful strategy for superior thermodynamics and hysteresis of Mg-Ni hydrogen energy storage alloys," *Journal of Alloys and Compounds*, vol. 766, pp. 112–122, 2018.
- [6] L. Yao, H. Han, Y. Liu, Y. Zhu, Y. Zhang, and L. Li, "Improved dehydrogenating property of polyvinylpyrrolidone coated Mg-Ni hydrogen storage nano-composite prepared by hydriding combustion synthesis and wet mechanical milling," *Progress in Natural Science: Materials International*, vol. 28, no. 1, pp. 7–14, 2018.
- [7] B. Dou, H. Zhang, and G. Cui, "Hydrogen sorption and desorption behaviors of Mg-Ni-Cu doped carbon nanotubes at high temperature," *Energy*, vol. 12, 2018.
- [8] Z. Lan, L. Zeng, G. Jiong et al., "Synthetical catalysis of nickel and graphene on enhanced hydrogen storage properties of magnesium," *International Journal of Hydrogen Energy*, vol. 44, no. 45, pp. 24849–24855, 2019.
- [9] Y. Li, J. Yang, L. Luo et al., "Microstructure characteristics, hydrogen storage kinetic and thermodynamic properties of  $Mg_{80}Ni_{20}Y$  ( $x = 0-7$ ) alloys," *International Journal of Hydrogen Energy*, vol. 44, no. 14, pp. 7371–7380, 2019.
- [10] B. P. Tarasov, A. A. Arbutov, S. A. Mozhuhin et al., "Hydrogen storage behavior of magnesium catalyzed by nickel-graphene nanocomposites," *International Journal of Hydrogen Energy*, vol. 44, no. 55, pp. 29212–29223, 2019.



- [11] H. Shao and X. Li, "Effect of nanostructure and partial substitution on gas absorption and electrochemical properties in  $Mg_2Ni$ -based alloys," *Journal of Alloys and Compounds*, vol. 667, pp. 191–197, 2016.
- [12] B. Aktekin, G. Çakmak, and T. Ozturk, "Induction thermal plasma synthesis of  $Mg_2Ni$  nanoparticles," *International Journal of Hydrogen Energy*, vol. 39, no. 18, pp. 9859–9864, 2014.
- [13] L. Zaluski, A. Zaluska, and J. O. StroM-Olsen, "Hydrogen absorption in nanocrystalline  $Mg_2Ni$  formed by mechanical alloying," *Journal of Alloys and Compounds*, vol. 217, no. 2, pp. 245–249, 1995.
- [14] P. Zolliker, K. Yvon, J. D. Jorgensen, and F. J. Rotella, "Structural studies of the hydrogen storage material magnesium nickel hydride ( $Mg_2NiH_4$ ). 2. Monoclinic low-temperature structure," *Inorganic Chemistry*, vol. 25, no. 20, pp. 3590–3593, 1986.
- [15] H. Yuan, H. Yang, Z. Zhou, D. Song, and Y. Zhang, "Pressure-composition isotherms of the  $Mg_{1.75}Ni_{0.75}Fe_{0.25}$ -Mg system synthesized by replacement-diffusion method," *Journal of Alloys and Compounds*, vol. 260, no. 1-2, pp. 256–259, 1997.
- [16] Q. M. Yang, Y. Q. Lei, C. P. Chen et al., "The thermal stability of amorphous hydride  $Mg_{50}Ni_{50}H_{54}$  and  $Mg_{30}Ni_{70}H_{45}$  \*," *Zeitschrift für Physikalische Chemie*, vol. 183, no. 1-2, pp. 141–147, 1994.
- [17] L. Zhang, S. M. Peng, and H. B. Yan, "Investigation of the preparation of  $Mg_2Ni$  nanocrystalline," *Journal of Materials Science and Engineering*, vol. 22, no. 4, p. 5, 2004.
- [18] H. Zoz, R. Reichardt, and H. Ren, *Energy Balance during Mechanical Alloying, Measurement and Calculation Method Supported by the, MALTOZ -software*, 1999.